Mathematical analysis of thermal diffusion shock waves

Vitalyi Gusev,[1] Walter Craig,[2] Roberto LiVoti,[3] Sorasak Danworaphong,[4] and Gerald J. Diebold[5]

[1]*Université du Maine, av. Messiaen, 72085 LeMans, Cedex 09 France*

[2]*Department of Mathematics, McMaster University, Hamilton, Ontario, Canada L8S 4K1*

[3]*Universita di Roma "La Sapienza," Dipartimento di Energetica, Via Scarpa, 14-00161 Roma, Italy*

[4]*School of Science, Walailak University, 222 Thaiburi, Thasala District, Nakorn Si Thammarat, 80160, Thailand*

[5]*Department of Chemistry, Brown University, Providence, Rhode Island 02912, USA*

Thermal diffusion, also known as the Ludwig-Soret effect, refers to the separation of mixtures in a temperature gradient. For a binary mixture the time dependence of the change in concentration of each species is governed by a nonlinear partial differential equation in space and time. Here, an exact solution of the Ludwig-Soret equation without mass diffusion for a sinusoidal temperature field is given. The solution shows that counterpropagating shock waves are produced which slow and eventually come to a halt. Expressions are found for the shock time for two limiting values of the starting density fraction. The effects of diffusion on the development of the concentration profile in time and space are found by numerical integration of the nonlinear differential equation.

I. INTRODUCTION

The separation of liquid mixtures in a thermal gradient was discovered by Ludwig [1] in 1856, and was described theoretically somewhat later by Soret [2]. The separation of mixtures by a thermal gradient takes place not only in liquids, but also in gases and solids, as is described by nonequilibrium thermodynamics [3–6]. Recently, a method of producing the Ludwig-Soret effect has been introduced where interference in the electric fields of two phase coherent light beams produces a temperature field with a sinusoidal component [7–10].

In this paper we discuss a solution to the Ludwig-Soret equation in a one-dimensional geometry for a sinusoidal temperature distribution. A derivation of an exact solution of the Ludwig-Soret problem with negligible mass diffusion is given in Sec. II. The time development of the shock fronts [11] are given in Sec. III. Section IV gives an expression for the shock velocity and expressions for the shock formation time for two limiting cases of the starting density fraction. Section IV also gives the effects of mass diffusion through numerical integration of the Ludwig-Soret equation and a derivation of the concentration profile in space at long times. The mathematical analysis given here presents considerably more detail than that given in Ref. [11], and includes the derivation of expressions for the shock formation time for two limiting cases.

II. SOLUTION TO THE THERMAL DIFFUSION EQUATION

Thermal diffusion in a binary mixture is governed by a pair of coupled differential equations [4] for the density fractions c_1 and c_2 of each species which obey the relation $c_1 + c_2 = 1$. If the temperature in a one-dimensional grating is given by $T = T_0[1 + \sin(Kx)]$, where $2T_0$ is the peak temperature, K is a wave number determined by the optical fringe spacing in the grating, and x is the coordinate and if the DuFour effect is neglected [4], then the coupled equations [12] yield a partial differential equation for one of the components,

$$\frac{\partial c(z,t)}{\partial \tau} = \alpha \frac{\partial}{\partial z}\{c(z,t)[1-c(z,t)]\cos z\} + \frac{\partial^2 c(z,t)}{\partial z^2}, \quad (1)$$

where c_2 has been written in terms of c_1, and the subscript 1 dropped from the density fraction c_1, where the thermal diffusion factor α, is defined as $\alpha = D'T_0/D$, where D' is the thermal diffusion coefficient and D is the mass diffusion coefficient, and where the dimensionless quantities τ and z are defined by $\tau = K^2 Dt$ and $z = Kx$.

As described in Ref. [12] if the last term in Eq. (1) describing diffusion is ignored, then the differential equation of motion for $c(z,t)$ can be written

$$\frac{\partial c}{\partial \tau} = -\frac{\partial f}{\partial z}, \quad (2)$$

where a "flux" $f(c,z)$ is defined as $f(c,z) = -\alpha c(1-c)\cos z$. Equation (2) is the differential form of a conservation equation that expresses the buildup of c in a volume as a consequence of a flux change in space. Since for a periodic temperature field the density fraction must also be periodic in z, it follows that $c(2\pi, \tau) = c(0, \tau)$. Integration of Eq. (2) over one period of the temperature field, i.e., from $z = 0$ to $z = 2\pi$, shows that the integral of c is independent of time and has a value of $2\pi c_0$, where c_0 is the density fraction at time $t = 0$, which expresses mass conservation for the Ludwig-Soret effect.

The Eulerian description of the profile $c = c(z, \tau)$ by Eq. (1) can be transformed [12] into a Lagrangian description yielding the coupled pair of ordinary differential equations,

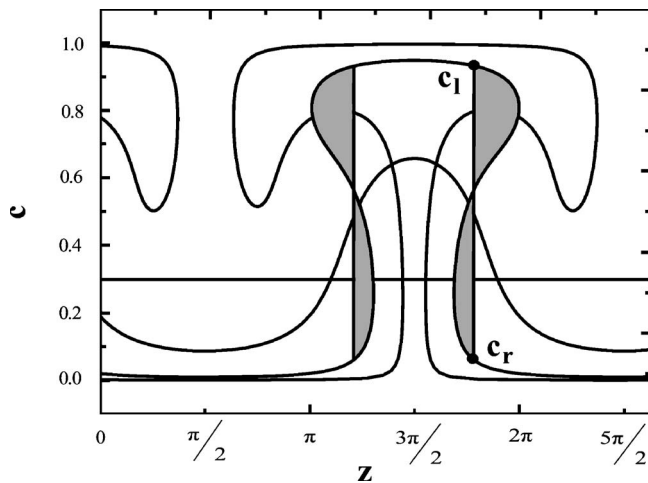$$\frac{dz}{d\tau} = \frac{\partial f(c,z)}{\partial c} = \alpha(2c-1)\cos z, \quad (3)$$

FIG. 1. Density fraction c versus dimensionless distance z for $\tau'=0$, 1.5, 3.5, and 6.0, for a starting density fraction $c_0=0.3$. The curves can be determined by numerical integration of Eqs. (3) and (4) or through solution of Eqs. (9) and (10). The vertical lines terminating at the density fractions c_r and c_l indicate the positions of the shock fronts. The shock position is found by determining the line that makes the areas of the shaded regions adjacent to each of the vertical lines equal.

$$\frac{dc}{d\tau} = -\frac{\partial f(c,z)}{\partial z} = -\alpha c(1-c)\sin z, \qquad (4)$$

that determine the motion of points with coordinates $z =z(\tau,c_0,z_0)$ and $c=c(\tau,c_0,z_0)$ on the zc plane for a point initially at (z_0,c_0) at time $\tau=0$. Numerical integration of Eqs. (3) and (4), which form a Hamiltonian system of equations [11,12] as found in classical mechanics, can be used to give the z coordinate and the value of c as a function of time for any point initially at (z_0,c_0), as shown in Fig. 1. From Eqs. (3) and (4) the slope of the curves on a phase portrait is found to be

$$\frac{dc}{dz} = -\frac{c(1-c)\sin z}{(2c-1)\cos z},$$

which can be written as

$$\frac{d}{dz}[c(1-c)\cos z] = 0. \qquad (5)$$

It follows then that the quantity in brackets in Eq. (5) is a constant, taken here to be k_1, so that

$$c(1-c)\cos z = k_1. \qquad (6)$$

The phase portrait for the Ludwig-Soret equation, as shown in Fig. 2, gives the trajectories of points with specified starting values of z and c. By differentiation of Eq. (6) with respect to c, it can be seen that the extreme values of the left hand side occurs when $\cos z=\pm 1$, and $c=1/2$; hence the values of k_1 are restricted to $|k_1|\leq 1/4$.

By solving Eqs. (4) and (6) for $\sin z$ and $\cos z$, respectively, and squaring and adding the resulting expressions, it is easily shown that

$$\left[\frac{k_1}{c(1-c)}\right]^2 + \left[\frac{1}{c(1-c)}\right]^2\left(\frac{dc}{d\tau'}\right)^2 = 1,$$

which can be written

$$\frac{dc}{\sqrt{c^2(1-c)^2-k_1^2}} = \pm d\tau', \qquad (7)$$

where the time variable τ' is defined as $\tau'=\alpha\tau$. Note that since c is restricted to the range $0<c<1$, real values of the left hand side of Eq. (7) are found only for $|k_1|\leq 1/4$. It is convenient to define the departure of the density fraction from a value of $1/2$ through the variable c', and to express the quantity in the denominator of Eq. (7) in terms of two parameters a and b, defined by
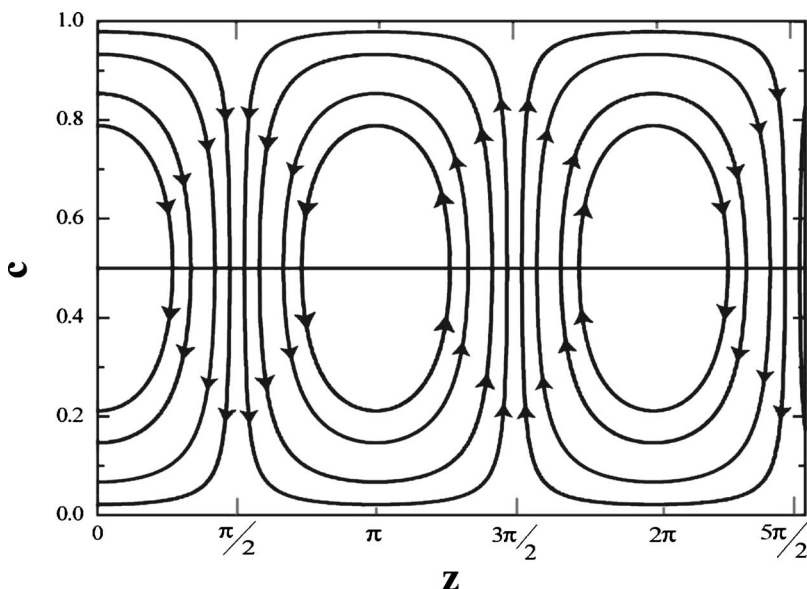
$$c' = c - \frac{1}{2},$$

FIG. 2. Phase portrait for the density fraction c versus dimensionless distance along the grating z from Eq. (6). Points on the zc plane move along curves of constant k_1 as time progresses.

$$a = \sqrt{\frac{1}{4} + |k_1|}, \quad b = \sqrt{\frac{1}{4} - |k_1|}.$$

Owing to the restriction on the magnitude of k_1, the inequality $a \geq b \geq 0$ is automatically satisfied. Hence Eq. (7) then can be integrated from a starting density fraction c_0 at time $\tau' = 0$ along a curve of constant k_1 to a density fraction c at time τ' giving

$$\int_{c_0 - 1/2}^{c - 1/2} \frac{dc'}{\sqrt{(a^2 - c'^2)(b^2 - c'^2)}} = \pm \int_0^{\tau'} d\tau'', \qquad (8)$$

where the integration is taken over a trajectory in phase space with a constant value of k_1. The left hand side of Eq. (8) can be expressed as an elliptic integral [13] of the first kind F, so that the solution to the Ludwig-Soret problem for a sinusoidal temperature field, neglecting diffusion, is

$$F\left[\arcsin\frac{c - \frac{1}{2}}{\sqrt{\frac{1}{4} - |k_1|}}, \frac{\frac{1}{4} - |k_1|}{\frac{1}{4} + |k_1|}\right]$$
$$- F\left[\arcsin\frac{c_0 - \frac{1}{2}}{\sqrt{\frac{1}{4} - |k_1|}}, \frac{\frac{1}{4} - |k_1|}{\frac{1}{4} + |k_1|}\right] = \pm \tau'\sqrt{\frac{1}{4} + |k_1|}. \qquad (9)$$

It can be seen that Eq. (9) gives τ' explicitly for any starting point (z_0, c_0) that arrives at the new point c; the new coordinate z is determined through

$$c_0(1 - c_0)\cos z_0 = c(1 - c)\cos z = k_1. \qquad (10)$$

From the point of view of calculating density fraction profiles as shown in Fig. 1, it is convenient to specify values of z_0, c_0 and τ' and to solve Eq. (9) for the new values of c through a numerical root search. Alternately, the points (c, z) can be substituted directly into Eq. (9) through use of Eq. (10) to determine k_1. Note that for positive values of α, the minus sign is used in Eq. (9) for points moving in the hot regions of the grating $0 < z < \pi$, and the plus sign is used for motion in the cold regions $\pi < z < 2\pi$, or $-\pi < z < 0$. Inversion of Eq. (9) to give c explicitly as a function of z for any given time τ', does not appear to be possible; however, it is straightforward to determine the profiles of the density fraction versus coordinate through numerical methods.

III. MOTION OF THE POINTS IN PHASE SPACE

Consider the motion of a point located between 0 and $\pi/2$ with a value of $c_0 < 1/2$. It can be seen from Figs. 1 and 3 that points in this region move downwards and towards the c axis. For such points the motion is determined first by Eq. (9) with a negative sign used, and after passing the c axis at $z = 0$, by Eq. (9) with the positive sign. Any point in this region starting at (z_0, c_0) reaches its minimum value c_{min} at $z = 0$, which from Eq. (10) is given by
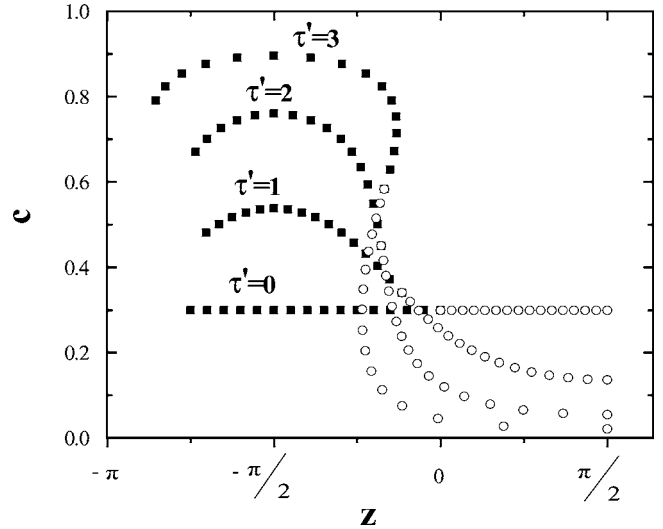

FIG. 3. Density fraction c versus dimensionless distance z from Eq. (13). with $\alpha = 1$ for $\tau' = 0$, 1, 2, and 3. The points plotted as circles ($\bigcirc$) are those that originally lie in the region $0 < z < \pi/2$ at $\tau' = 0$. The points plotted as squares ($\blacksquare$) are those that lie in the region $-\pi/2 < z < 0$ at time $\tau' = 0$. The starting density fraction is 0.3.

$$c_{min} = \frac{1}{2} - \sqrt{\frac{1}{4} - c_0(1 - c_0)\cos z_0}. \qquad (11)$$

The time required to arrive at c_{min} is therefore

$$\tau'_{min} = -\int_{c_0}^{c_{min}} \frac{dx}{\sqrt{x^2(1 - x)^2 - [c_0(1 - c_0)\cos z_0]^2}}, \qquad (12)$$

and the total time τ', from the starting point to the point (z, c) is

$$\tau' = \tau'_{min} + \int_{c_{min}}^{c} \frac{dx}{\sqrt{x^2(1 - x)^2 - [c_0(1 - c_0)\cos z_0]^2}} \qquad (13)$$

which can be written in terms of elliptic integrals as in Eq. (9). Since the shocks in the region $-\pi/2 < z < 0$ originate from initial points in the region $0 > z < \pi/2$, Eq. (13) is an expression that can be used to determine the time of shock formation.

Similar reasoning gives the maximum density fraction c_{max} for any point starting at (c_0, z_0) located between 0 and $\pi/2$ as

$$c_{max} = \frac{1}{2} + \sqrt{\frac{1}{4} - c_0(1 - c_0)\cos z_0}, \qquad (14)$$

where τ'_{max}, the time it takes to move from c_0 to c_{min} to c_{max}, is given by

$$\tau'_{max} = \tau'_{min} + \int_{c_{min}}^{c_{max}} \frac{dx}{\sqrt{x^2(1 - x)^2 - [c_0(1 - c_0)\cos z_0]^2}}. \qquad (15)$$

The curves in Fig. 3 show how points originally in the region between 0 and $\pi/2$ move downwards to their minimum val-

ues at $z=0$, pass to the left of the c axis, and then rise upwards as time progresses.

IV. SHOCK FORMATION

A. Determination of the shock velocity

It is clear from examination of Figs. 1 and 2 that the solutions to Eq. (9) become mutivalued, i.e., nonfunctional, after a certain time. Similar solutions to Eq. (9) for different values of c_0 show that nonfunctional behavior is found for any value of c_0, with the largest values of the shock formation time being found for the smallest initial density fractions c_0. When the slope of any solution for c on the zc plane becomes unbounded, i.e., immediately before the density fraction profile becomes multivalued, the solution to Eqs. (3) and (4) must be treated as describing a shock. At later time, the vertical, i.e., shock, part of the concentration profile is introduced in accordance with the mass conservation law.

The formation of a shock indicated by the vertical line in Fig. 1 at $\tau'=3.5$, terminated by c_l on the left and c_r on the right, eliminates the multivalued dependence of c on z. As τ' continues to increase (for $d\tau'>0$) from its value of 3.5, points on the shock situated above $c=1/2$ move to the right along the z axis while those points below $c=1/2$ move towards the left, as can be seen in Fig. 2. As the time progresses to $\tau'=3.5+d\tau'$ the nonfunctionality of the solution for c must be once again eliminated by installing a new vertical shock front, but in a position shifted along the z axis by dz_{sh} relative to its position at $\tau'=3.5$. The condition that the installation of the shock does not change the area under the density fraction profile in the zc plane can be written as

$$dz_{sh}(c_l - c_r) = \int_{c_r}^{c_l} dz(c)dc$$

or

$$\frac{dz_{sh}}{d\tau'}(c_l - c_r) = \int_{c_r}^{c_l} \frac{dz}{d\tau'}dc$$

which, together with Eq. (3), gives

$$\frac{dz_{sh}}{d\tau}(c_l - c_r)d\tau = \alpha \cos z \int_{c_r}^{c_l} (2c - 1)dc. \quad (16)$$

After evaluation of the integral in Eq. (16) the shock velocity $dz_{sh}/d\tau$ becomes

$$\frac{dz_{sh}}{d\tau} = \alpha(c_l + c_r - 1)\cos z. \quad (17)$$

It can be seen that two shocks, one on either side of the point $z=3\pi/2$ are formed, each of which travels with the same speed towards the cold region of the grating, the different velocities being determined by the change in sign of the cosine function on either side of $z=3\pi/2$. The left-going shock comes to a halt when $c_l=1$ and $c_r=0$, that is, where a complete separation of the mixture has been attained, at which point the profile of c in space is a square wave centered at $z=3\pi/2$.
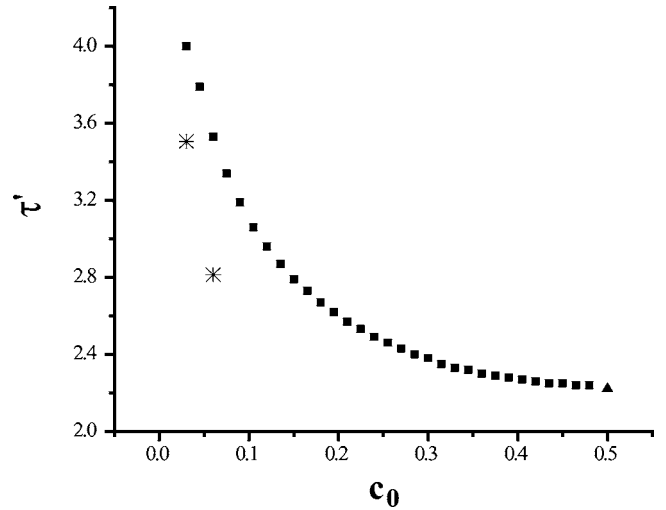

FIG. 4. Time for formation of a shock τ' versus the starting density fraction c_0 from numerical integration of the Hamiltonian system of equations. The point (▲) at $c_0 \cong 1/2$, is the limiting value of τ' from Eq. (25). The points (∗) are from Eq. (27) for $c_0 \cong 0$.

Note that the shock velocity can be obtained equally by writing Eq. (3) as $dz_{sh}/d\tau = [f(c_l,z) - f(c_r,z)]/(c_l - c_r)$, which, after substitution of the expression for the flux function, gives Eq. (17). As noted in Ref. [11], Eq. (17), which expresses the thermal diffusion shock velocity in terms of density fractions on either side of the shock, is an exact analog of the Rankine-Hugoniot relations for one-dimensional fluid shocks: Eq. (17) gives the thermal diffusion shock speed in terms of the "state variables" c_l and c_r, the Rankine-Hugoniot relations express the shock speed in terms of ratios of the state variables of the fluid on either side of the shock.

The time of formation of the shock can be found from numerical integration of the Hamiltonian system of equations and finding the point in space and time where the profile becomes multivalued. Figure 4 shows a plot of the dimensionless time τ' required for shock formation versus the initial density fraction c_0 found from Eqs. (3) and (4).

B. Shock formation time: $c_0 \lesssim 1/2$

Consider the region between $-\pi/2$ and $\pi/2$. When c_0 is approximately equal to $1/2$, the shock must form at a point to the left of $z=0$, but near the point $z=0$. If the cosine function is approximated as $\cos z \cong 1 - z^2/2$ and substituted into Eq. (6) then the trajectories shown in Fig. 2 reduce to circles described by

$$\left(\frac{z}{2\sqrt{2}}\right)^2 + c'^2 = \frac{1}{4} - k_1 \quad (18)$$

on the zc plane for $k_1 \leq \frac{1}{4}$. Substitution of z from Eq. (18) into Eq. (4) with the sine function approximated as $\sin z \cong z$ gives

$$\frac{dc'}{\sqrt{\frac{1}{4} - k_1 - c'^2}} = \pm \frac{d\tau'}{\sqrt{2}}, \quad (19)$$

which can be integrated to give

$$\arcsin\left(\frac{c'}{\sqrt{\frac{1}{4}-k_1}}\right) - \arcsin\left(\frac{c_0'}{\sqrt{\frac{1}{4}-k_1}}\right) = \frac{\tau'}{\sqrt{2}}, \quad (20)$$

for points initially in the region $z < 0$. Further manipulation of Eq. (20) gives for $z < 0$,

$$\frac{c'\sqrt{c'^2 - c_0'^2 + z^{\dagger2}} + c_0' z^{\dagger}}{c'^2 + z^{\dagger2}} = \sin \tau^{\dagger}, \quad (21)$$

where $z^{\dagger}$ has been defined as $z^{\dagger} = z/2\sqrt{2}$ and $\tau^{\dagger} = \tau'/\sqrt{2}$. It is convenient at this point to express the coordinates c' and $z^{\dagger}$ in Eq. (21) in cylindrical coordinates, $c' = -r\cos\phi$ and $z^{\dagger} = -r\sin\phi$, where ϕ is an angle measured clockwise with respect to the negative c axis. Equation (21) gives, after some algebraic manipulation,

$$r = -c_0' \frac{\cos(\phi + \tau^{\dagger})}{\cos^2\phi - \sin^2\tau^{\dagger}} \quad (22)$$

for points initially in the region $-\pi/2 \leq z \leq 0$. The modified density fraction c' and coordinate $z^{\dagger}$ then become

$$z^{\dagger} = c_0' \frac{\cos(\phi + \tau^{\dagger})}{\cos^2\phi - \sin^2\tau^{\dagger}} \sin \phi,$$

$$c' = c_0' \frac{\cos(\phi + \tau^{\dagger})}{\cos^2\phi - \sin^2\tau^{\dagger}} \cos \phi. \quad (23)$$

The condition for the appearance of a shock is that $dz^{\dagger}/dc'$ should approach zero, which from Eqs. (23) can be found as

$$\frac{dz^{\dagger}}{dc'} = \frac{\cos(2\phi + \tau^{\dagger})[\cos^2\phi - \sin^2\tau^{\dagger}] + \sin(2\phi)\cos(\phi + \tau^{\dagger})\sin \phi}{\sin(2\phi)\cos(\phi + \tau^{\dagger})\sin \phi - \sin(2\phi + \tau^{\dagger})[\cos^2\phi - \sin^2\tau^{\dagger}]}. \quad (24)$$

The shock for c_0' approximately equal to zero is expected to appear at $\phi = \pi$ so that Eq. (24) reduces to $dz^{\dagger}/dc' = -\cot\tau^{\dagger} = 0$; hence it follows that $\tau^{\dagger} = \pi/2$, and the time for shock formation is

$$\tau' \simeq \frac{\pi}{\sqrt{2}}. \quad (25)$$

As can be seen in Fig. 4 the shock time given by Eq. (25) is in excellent agreement with the numerical results.

C. Shock formation time: $c_0 \cong 0$

A second case where the time of shock formation time can be found in closed form is when the initial density fraction is small. Consider points in the region $-\pi/2 < z < \pi/2$. Starting from Eq. (13), the time for the density fraction to reach a value c starting from the point (z_0, c_0) can be shown to be given by

$$\tau' = \int_{c_0}^{c} \frac{dx}{\sqrt{x^2(1-x)^2 - c_0^2(1-c_0)^2\cos^2 z_0}}$$

$$+ 2\int_{c_{\min}}^{c_0} \frac{dx}{\sqrt{x^2(1-x)^2 - c_0^2(1-c_0)^2\cos^2 z_0}}. \quad (26)$$

It is clear from plots found from the solution to Eq. (13) or through numerical integration of Eqs. (3) and (4) that the points first forming the shock lie originally in the region $0 < z < \pi/2$ and which move downward and to the left along the curves shown in Fig. 2. For small c_0, the shock forms at values of $c \simeq 1/2$ near $-\pi/2$ from points z_0 on the positive z axis where $z_0 \simeq 0$. Equation (26) can then be approximated as

$$\tau' \simeq \int_{c_0}^{1/2} \frac{dx}{\sqrt{x^2 - c_{\min}^2}} + 2\int_{c_{\min}}^{c_0} \frac{dx}{\sqrt{x^2 - c_{\min}^2}}$$

giving τ' as

$$\tau' \simeq -\ln c_0 + \ln\left(\frac{c_0 + \sqrt{c_0^2 - c_{\min}^2}}{c_{\min}}\right),$$

where $c_{\min} \simeq c_0\cos z_0$. Since the shock is formed by points initially in the region $z_0 \simeq 0$, the time for the shock to form for small c_0 is thus

$$\tau' \simeq -\ln c_0. \quad (27)$$

The plot in Fig. 4 gives two points from Eq. (27). Evaluation of the shock time for values smaller than those given in Fig. 4 shows that the approximation given by Eq. (27) gets successively better for small values of c_0. For example, for $c_0 = 5 \times 10^{-5}$, numerical integration gives $\tau' = 10.6$ whereas Eq. (27) gives $\tau' = 9.9$.

V. EFFECTS OF MASS DIFFUSION

A. Results from numerical integration

The effects of mass diffusion were determined by numerical integration of Eq. (1) using the finite difference method, which gives a solution by considering small changes in the density fraction resulting from a change in time $\Delta\tau$ and space Δz. A solution for c is obtained by selecting successively smaller values of $\Delta\tau$ and Δz until the solution converges. The first order derivative of the density fraction with respect to z at a time t_k at the point z_k is given, for instance, by
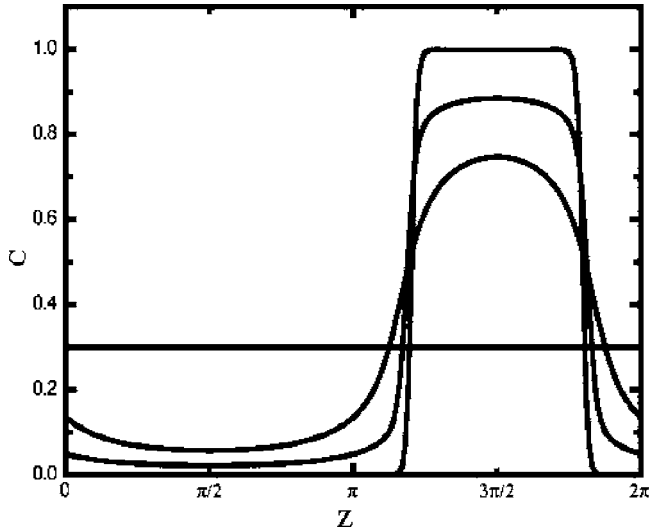
FIG. 5. Density fraction c versus dimensionless distance z for $\alpha = 40$. The times for the plots are $\tau' = 0$, 0.20, 0.40, and 1.08 for plots with successively higher peak values of c.

$$\frac{\partial c}{\partial z} = \frac{c(t_k, z_{i+1}) - c(t_k, z_{i-1})}{2\Delta z}. \tag{28}$$

Since derivatives must be computed at the end points of the integration range in space, the periodicity of the solution is used to give values for the required derivatives. The modulus function $\mathrm{mod}(a,b)$ is introduced to represent the remaining integer of division of a by b. For example, $\mathrm{mod}(3,2)$ is equal to 1 and $\mathrm{mod}(4,2)$ is equal to zero. If a is less than b, the value of the modulus function is a, where a is a positive integer, including zero. The expressions for the first and second space derivatives become

$$\frac{\partial c}{\partial z} = \frac{c(t_k, z_{\mathrm{mod}(i+1,i_{\max})}) - c(t_k, z_{\mathrm{mod}(i-1,i_{\max})})}{2\Delta z},$$

$$\frac{\partial^2 c}{\partial z^2} = \frac{c(t_k, z_{\mathrm{mod}(i+1,i_{\max})}) - 2c(t_k, z_i) + c(t_k, z_{\mathrm{mod}(i-1,i_{\max})})}{\Delta z^2}.$$

To simplify the notation, z_i and τ_k are now replaced by their indices, giving Eq. (1) as

$$c(k+1,i) = c(k,i) + \alpha_T \Delta \tau \cos\left(2\pi \frac{i}{i_{\max}}\right)[1 - 2c(k,i)]$$

$$\times \left[\frac{c(k,\mathrm{mod}(i+1,i_{\max})) - c(k,\mathrm{mod}(i-1,i_{\max}))}{2\Delta z}\right]$$

$$- \alpha_T \Delta \tau \left[\sin\left(2\pi \frac{i}{i_{\max}}\right)[c(k,i) - c^2(k,i)]\right]$$

$$+ \left(\frac{\Delta \tau}{\Delta z^2}\right) \times [c(k,\mathrm{mod}(i+1,i_{\max})) - 2c(k,i)$$

$$+ c(k,\mathrm{mod}(i-1,i_{\max}))]. \tag{29}$$

The plots shown in Fig. 5 indicate that the effect of diffusion is to remove the high spatial frequencies in the distribution. Since the spatial profile of c depends on α and τ'

only, it is possible to calculate the spatial Fourier components of the distribution after obtaining c from numerical integration, and hence to determine the intensity of light diffracted from an absorption grating, as was done in Ref. [11]. By minimizing the error in a fit to the intensities of the diffracted light beams, the thermal diffusion factor can be determined from experimental data.

B. Density fraction distribution for long times

When τ' becomes long, thermal diffusion is exactly balanced by mass diffusion and the spatial profile of the density fraction must approach a limiting form. It can be seen that when $dc/d\tau' = 0$, Eq. (1) reduces to an ordinary differential equation in z, a first integral of which is given by

$$\frac{dc}{dz} + \alpha c(1-c)\frac{d\hat{T}}{dz} = C, \tag{30}$$

where C is a constant, and a dimensionless spatial derivative of the temperature field $d\hat{T}/dz$ has been substituted for the cosine function. For temperature fields that are periodic in z it is expected that in the region $0 < z < 2\pi$, both dc/dz and $d\hat{T}/dz$ will be zero at the same value of z. For the present problem, both of these quantities are zero at the point $z = 3\pi/2$; hence the constant C must be zero and Eq. (30) can be integrated as

$$\int_{c(z_0)}^{c(z)} \frac{dc}{c(1-c)} = -\alpha \int_{z_0}^{z} \frac{d\hat{T}}{dz} dz. \tag{31}$$

The general solution to Eq. (31) is thus

$$c(z) = \frac{1}{1 + Fe^{\alpha T(z)}}, \tag{32}$$

where F is a constant given by $[1-c(z_0)]\exp[-\alpha\hat{T} \times (z_0)]/c(z_0)$. For the present problem with a sinusoidal temperature field, the long time distribution becomes

$$c(z) = \frac{1}{1 + Fe^{\alpha \sin z}}. \tag{33}$$

An equivalent expression for the linearized Eq. (1) has been given in Ref. [12]. Since the value of $c(z_0)$ is not known without solution to Eq. (1), $F(\alpha, c_0)$ can be determined for a given value of α and c_0 through use of the mass conservation law. Depending on the value of α, curves of c versus α from Eq. (33) can resemble a sinusoidal function for small α, or a nearly square wave for large α.

VI. DISCUSSION

The expressions in Eqs. (9) and (13) provide an exact solution to the thermal diffusion problem without mass diffusion. If Eq. (1) is divided by α so that the time derivative is expressed with respect to τ', it is clear that the effects of diffusion are small when α is large or when the gradient of the density fraction is small, such as at short times. The conditions for the time of appearance of the shocks is

straightforward, however, closed form expressions for the shock formation time have been found only in two limiting cases.

The formation of shocks follows from the nonlinearity of the dependent variable c in Eq. (1). Perhaps the unique feature of shocks produced by thermal diffusion in sinusoidal temperature fields is that they come as counterpropagating pairs of waves, the direction of which is governed by the sign of the cosine function in Eq. (17) to the right and left of $z=3\pi/2$. The left-going wave near $z=3\pi/2$ has the property that it slows to a speed of zero when c_l approaches 1, and c_r approaches zero. At this point in time, a complete separation of the mixtures, possible only in the absence of diffusion, takes place.

The parallel between thermal diffusion shocks and fluid shocks has been given in Ref. [11]. In both cases, the mathematics are treated by ignoring the dissipative term in the equations of motion to find the properties of the shock waves. In fluid shocks, viscosity causes a broadening of the shock front, just as mass diffusion broadens the thermal diffusion shock fronts, as shown by the results of numerical integration given here. The extent to which thermal diffusion shocks are visible in the laboratory is clearly a function of how large the thermal diffusion factor can be made.

[1] C. Ludwig, Sitzber. Akad. Wiss. Vien Math.-naturw. **20**, 539 (1856).

[2] C. Soret, Arch. Sci. Phys. Nat. **3**, 48 (1879).

[3] D. D. Fitts, *Nonequilibrium Thermodynamics* (McGraw-Hill, New York, 1962).

[4] S. R. deGroot and P. Mazur, *Non-Equilibrium Thermodynamics* (North-Holland, Amsterdam, 1962); as noted in this reference the Dufour effect is generally small and can be ignored.

[5] E. A. Mason, R. J. Munn, and R. J. Smigh, in *Advances in Atomic and Molecular Physics*, edited by D. R. Bates (Academic Press, New York, 1966), p. 33.

[6] R. D. Present, *Kinetic Theory of Gases* (McGraw-Hill, New York, 1958).

[7] K. Thyagarajan and P. Lallemand, Opt. Commun. **36**, 54 (1978).

[8] F. Bloisi, Opt. Commun. **68**, 87 (1988).

[9] W. Köhler, J. Chem. Phys. **98**, 660 (1993).

[10] W. Köhler and S. Wiegand, in *Thermal Nonequilibrium Phenomena in Fluid Mixtures*, edited by W. Köhler and S. Wiegand (Springer-Verlag, Berlin, 2001), p. 190.

[11] S. Danworaphong, W. Craig, V. Gusev, and G. J. Diebold, Phys. Rev. Lett. **94**, 095901 (2005).

[12] W. L. Craig, S. Danworaphong, and G. J. Diebold, Phys. Rev. Lett. **92**, 125901 (2004).

[13] *Handbook of Mathematical Functions with Formulas, Graphs, and Mathematical Tables*, edited by M. Abramowitz and I. Stegun (National Bureau of Standards, Washington, DC, 1964), Vol. 55, p. 596; some authors [e.g., I. Gradshteyn and L. Ryzhik, *Table of Integrals, Series, and Products* (Academic Press, New York, 1980) give the elliptic integral with the second argument as b/a instead of b^2/a^2. We believe the latter to be correct].